Article

$^{40}Ar/^{39}Ar$ Geochronology of the Malyy (Little) Murun massif, Aldan Shield of the Siberian Craton: a simple story for an intricate igneous complex

Alexei V. Ivanov [1,*], Nikolay V. Vladykin [2], Elena I. Demonterova [1], Viktor A. Gorovoy [1], Emilia Y. Dokuchits [2]

[1] Institute of the Earth's Crust, Siberian Branch of the Russian Academy of Sciences, Irkutsk, Russia; aivanov @crust.irk.ru

[2] A.P. Vinogradov Institute of Geochemistry, Siberian Branch of the Russian Academy of Sciences, Irkutsk, Russia; vlad@igc.irk.ru

* Correspondence: aivanov @crust.irk.ru; Tel.: +7-395-242-7000

Abstract: The Malyy (Little) Murun massif of the Aldan Shield of the Siberian Craton has long been a kind of the geologists' Siberian Mecca. It attracted thousands of geologists, prospectors and mineral collectors despite of its remote location. It is famous for a dozen of new and rare minerals, including gemstones charoite and dianite (the latter is the market name for strontian potassicrichrerite), as well as for specific alkaline igneous rocks. Despite of this, the age of the Malyy Murun igneous complex and associated metasomatic and hydrothermal mineral associations remained poorly constrained. In this paper, we provide extensive $^{40}Ar/^{39}Ar$ geochronological data to reveal its age and temporal history. It appeared that being unique in terms of rocks and constituent minerals, the Malyy Murun is one of multiple alkaline massifs and lavas emplaced in Early Cretaceous (~137-128 Ma) within a framework of extensional setting of the Aldan Shield and nearby Transbaikalian region. The extension has occurred 40-60 million years after the supposed closure of the Mongolia-Okhotsk Ocean and peak of orogeny in Early-Middle Jurassic.

Keywords: Malyy (Little) Murun massif; Aldan Shield; Siberian Craton; $^{40}Ar/^{39}Ar$ dating

1. Introduction

The Malyy (Little) Murun massif of the Aldan Shield of the Siberian Craton (Fig. 1), though located in the remote Siberia, is familiar to several generations of Russian geologists and to international community due to specific assemblage of alkaline igneous rocks [1-16] and mineral deposits for U, Th, Au, Pb, Ti, Sr and Ba associated with intrusive and post-intrusive stages of this massif [12-19]. At last, but not least, the Malyy Murun massif is famous for the only world occurrence of gemstone charoite [20-24].

In 1980-s, up to several thousand of geologists and miners worked at the Malyy Murun massif during the short Siberian summers in search for various metal and non-metal resources. Today, only limited mining operations are conducted there for the gemstone market (charoite, dianite – the market name for strontian potassicrichrerite [24]) and metallurgy (Ba-Sr benstonite carbonatite [12-14]). The Malyy Murun has high potential for mineralogists and petrologists. Worth to mention a number of new minerals and mineral varieties discovered there (charoite [20, 25], tinaksite [26-27], tokkoite [27-28], frankamenite [29-30], strontian potassicrichrerite [31-32], tausonite [33-34], murunskite [35-36], vladykinite [37]) and various exotic rocks such as lamproites, carbonatites, alkaline granites and various syenitic rocks.

Despite the enormous efforts for understanding geology of the Malyy Murun massif, its geochronology was constrained to Early Cretaceous by an outdated K-Ar dating of voluminously predominant syenites [38]. A few attempts were also made recently to limit the timing of the charoite mineralization by $^{40}Ar/^{39}Ar$ dating [39-40]. In this study, we provide new $^{40}Ar/^{39}Ar$ results on all major

igneous and hydrothermal stages recognized in the Malyy Murun massif. We use this geochronological information to constrain the duration of magmatic and later hydrothermal activity within the massif and to compare it with the information on alkaline magmatism of the Aldan Shield of the Siberian Craton and Transbaikalian rifted region (Fig. 1).

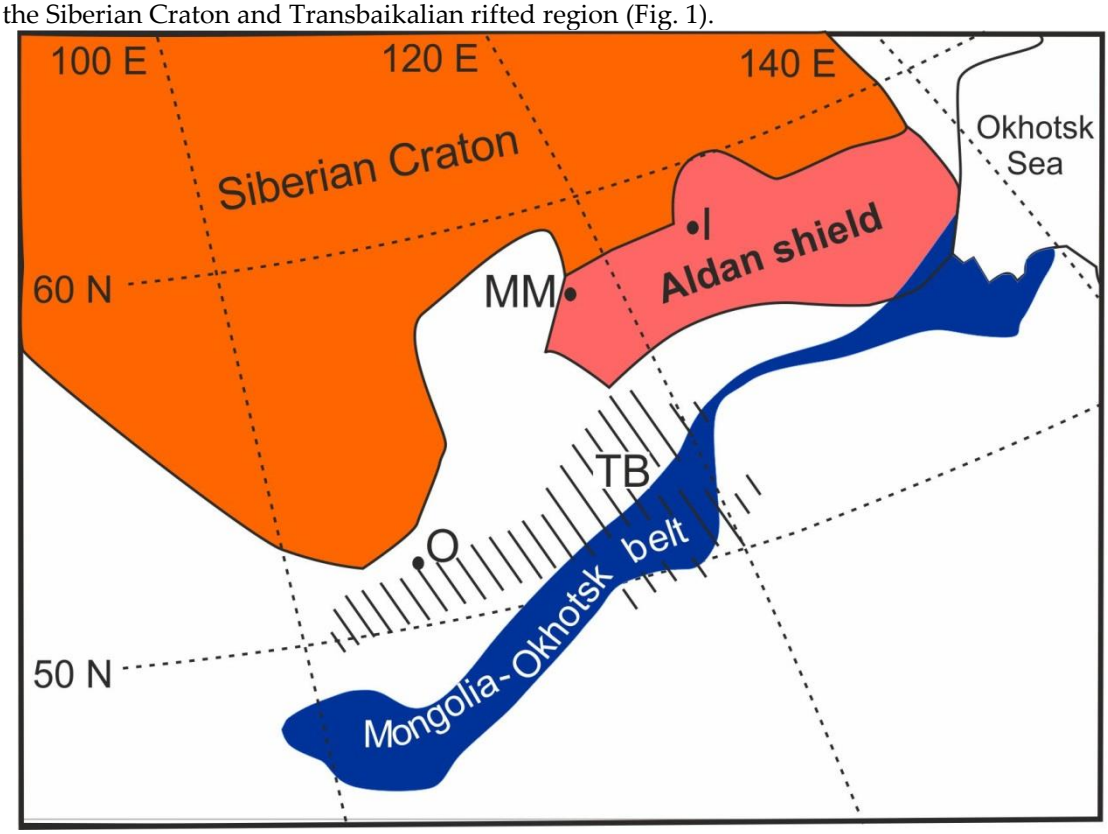

Figure 1. Location of the Malyy Murun and some other alkaline complexes in the tectonic framework of the Siberian Craton and the Mongolia-Okhotsk belt (after [39]). MM - Malyy Murun, I – Inagly, O – Oshurkov. The latter is a Jurassic orogen formed due to the closure of an ocean of the same name. Aldan Shield is the cratonic basement intruded by numerous Cretaceous small volume alkaline intrusions [38]. TB (hatched) is a Transbaikalian region rifted in Cretaceous with formation of basins and associated alkaline basaltic volcanism [53].

2. Materials and Methods

According to [15], the Malyy Murun massif can be subdivided into four igneous phases or stages (early intrusive, main intrusive, volcanic and late intrusive). Relation between different igneous stages were not always clear because the rocks classified to one or another of the four stages are usually separated by faults and no direct contacts can be observed for all rock types to establish the complete scheme based purely on geological relationships. Thus it is not surprising that other subdivisions can be found in literature (e.g. [22]). Here we follow the subdivision of [15], though slightly modify it as indicated below.

Rocks of the early intrusive stage are predominantly located in the northeastern part of the massif (Fig. 2), where they were recovered through drilling and mining of an exploratory gallery. Biotite-pyroxenites, K-ijolites, olivine lamproites, feldspar-shonkinites, leucitic shonkinites and cumulative olivine-spinel and olivine-pyroxene-phlogopite-monticellite rocks form a layered complex. For geochronological purpose, mica was separated from biotite-pyroxenite, olivine lamproite and olivine-pyroxene-phlogopite-monticellite rock (Appendix A).

Rocks of the main intrusive stage compose the central part of the massif (Fig. 2), which consists of different types of syenites (leucitic, feldspar-calcilitic, biotite-pyroxene-K-feldspar). For $^{40}Ar/^{39}Ar$ dating we separated mica from abundant biotite-pyroxene-K-feldspar syenite (referred to as alkaline syenite by Russian geologists).

Preprints (www.preprints.org) | NOT PEER-REVIEWED | Posted: 19 November 2018 doi:10.20944/preprints201811.0470.v1

Peer-reviewed version available at Minerals 2018, 8, 602; doi:10.3390/min8120602

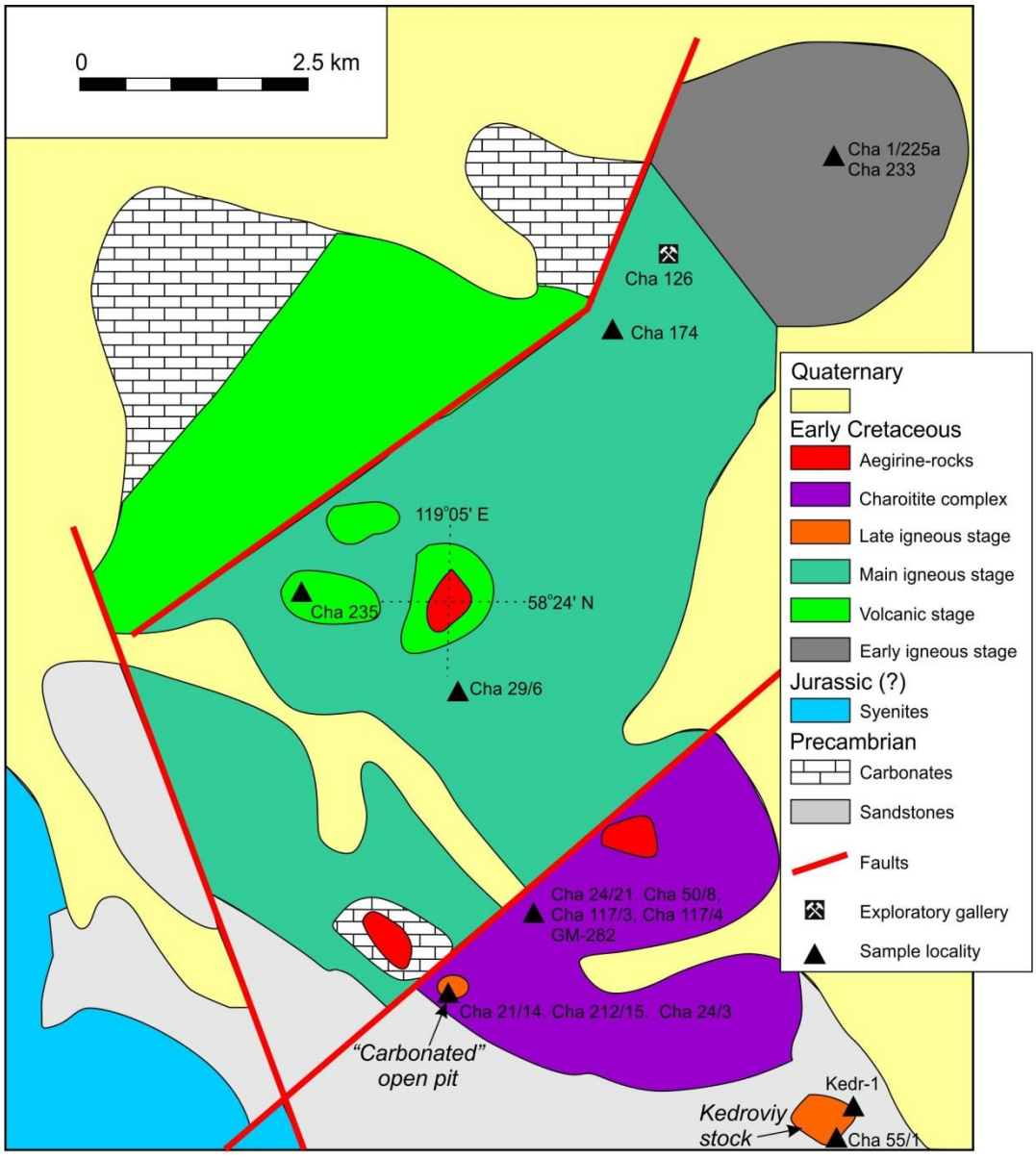

Figure 2. A schematic map of the Malyy Murun massif with location of the studied samples.

Volcanic stage is recognized by lava of leucitic lamproites and melaphonolites and volcanic breccia. The latter includes clasts of rocks of the main intrusive stage. Dykes of tinguaites, richterite-sanidine lamproites, trachyte-porphyries, syenite-porphyries and (eudialyte-bearing) lujavrites are included into the volcanic stage. For $^{40}Ar/^{39}Ar$ dating we separated mica from leucitic lamproite lava and lujavrite dyke.

According to [15], the late intrusive stage includes benstonite, calcite and quartz-calcite carbonatites (Fig. 3) and various types of silicate-carbonate rocks (with variable content of K-feldspar, pyroxene and calcite) spatially associated with charoitites (Fig. 4). For the purpose of this study, we keep carbonatites as the true representatives of the late intrusive stage, whereas consider other silicate-carbonate and silicate rocks (often referred to as fenites [e.g. 22]) within the charoite complex (Fig. 2). In addition, we include into the late intrusive stage alkaline granites of spatially separated Kedroviy stock (Fig. 2), which were considered within the main intrusive stage [15] or a late stage [22]. For $^{40}Ar/^{39}Ar$ dating of the late intrusive stage, we separated tinaksite and K-feldspar from benstonite carbonatite and K-feldspar from calcite carbonatite. In order to obtain the age constraints on alkaline granites of the Kedroviy stock, we separated alkaline amphibole (strontian potassicrichrerite [31]) from a metasomatic contact zone.

Preprints (www.preprints.org) | NOT PEER-REVIEWED | Posted: 19 November 2018 doi:10.20944/preprints201811.0470.v1

Peer-reviewed version available at Minerals 2018, 8, 602; doi:10.3390/min8120602

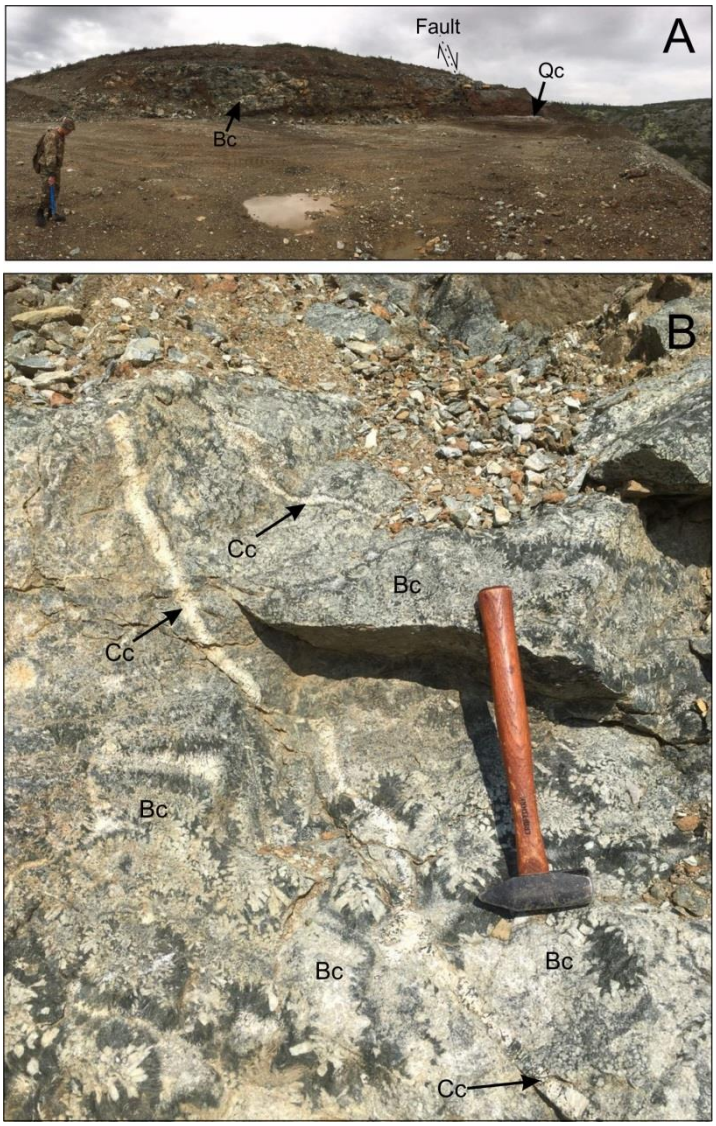

Figure 3. The "Carbonated" open pit: (A) a general view with shown sites of benstonite carbonatite (Bc) and quartz carbonatite (Qc) blocks separated by a fault, (B) a close view to benstonite carbonatite (Bc) cut by calcite carbonatite (Cc) veins.

Hydrothermal activity within and in vicinity of the Malyy Murun massif is represented by quartz veins, which commonly contain rutile - brookite – anatase ore grade mineralization [19]. For $^{40}Ar/^{39}Ar$ dating we collected K-feldspar from one of such veins within the Kedroviy stock.

For dating of the charoitite complex, we separated K-feldspar from charoitite and K-feldspar from a microcline monomineralic vein (Fig. 4). In addition to this we use own published data [40] for K-feldspar from a museum sample, which likely was collected from massive K-feldspar (microcline) monomineralic rock. We also collected rare minerals such as frankamenite, tinaksite, tokkoite and K-arvfedsonite, taken from field samples and museum collections.

$^{40}Ar/^{39}Ar$ dating was performed at the Centre for Geodynamics and Geochronology at the Institute of the Earth's Crust, Siberian Branch of the Russian Academy of Sciences (Irkutsk, Russia). The analytical procedure was published elsewhere [e.g. 41], thus only a brief description is given here. The instrument used was a noble-gas mass-spectrometer ARGUS VI (Thermo Fisher Scientific) equipped with a double-vacuum resistance oven and a gas cleaning system with few SAES-getters. Ages were calculated using the conventional decay constants [42] and a revised atmospheric $^{40}Ar/^{36}Ar$ ratio of 298.56 [43]. J-factor was derived from measurements of BERN-4M monitor located between every 3-4 unknown-age samples. In order to make the $^{40}Ar/^{39}Ar$ calculated age values consistent with the U-Pb-based geochronological scale (i.e. ~1% older [44-46]) we assigned to BERN-4M an age of 18.885 Ma [47]. Age values are calculated using Isoplot macros for Excel [48] in stepwise heating

Preprints (www.preprints.org) | NOT PEER-REVIEWED | Posted: 19 November 2018 doi:10.20944/preprints201811.0470.v1

Peer-reviewed version available at Minerals 2018, 8, 602; doi:10.3390/min8120602

diagram and inverse isochron coordinates ($^{36}Ar/^{40}Ar$ vs $^{39}Ar/^{40}Ar$). We define plateau as 4 or more consecutive steps within analytical error which account for >60% of released ^{39}Ar and whose age values overlaps within an error with an age value derived by inverse isochron for the same steps. If one of the criteria above is not met, for example 4 or more steps with <60% of released ^{39}Ar, we consider such part of the argon released spectrum as a sub-plateau, reliability of which is discussed for each case individually. If no part of the argon released spectrum can be considered as plateau or sub-plateau, we calculate an average as an approximate estimate of age. If an isochron intersects with the $^{36}Ar/^{40}Ar$ axis at non-atmospheric ratio we prefer the isochron over the plateau. In other cases, the plateau age value is preferred as the true estimate of the emplacement age. A summary of geochronological results is provided in Appendix A.

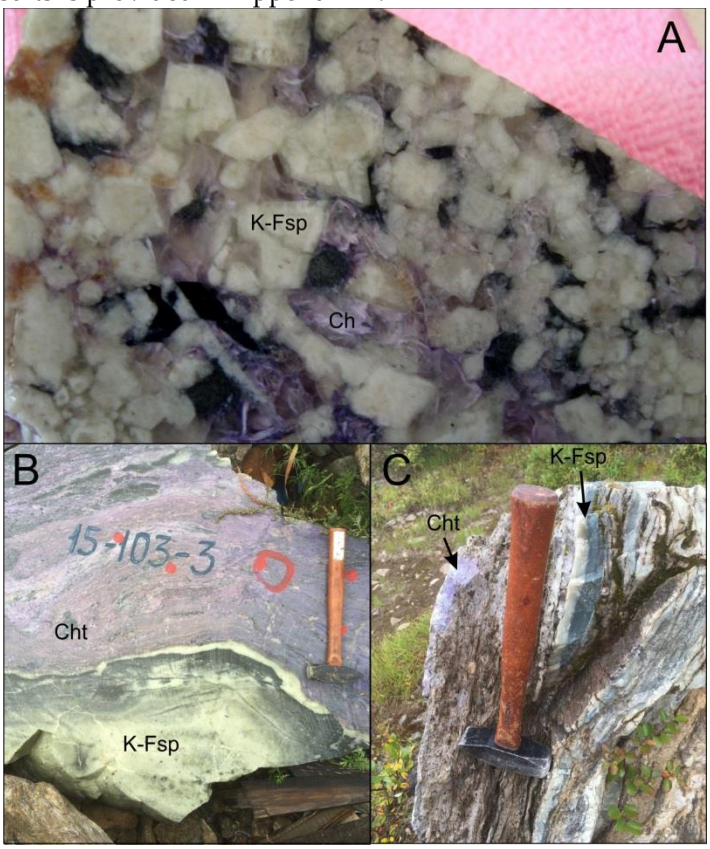

Figure 4. Different types of K-feldspar-bearing (microcline) rocks: (A) a polished hand specimen (~20 cm in long direction) of granular microcline (K-Fsp) in intergrowth with charoite (Ch), (B) a large xenolith of a massive monomineralic microcline rock (K-Fsp) within charoitite (Cht) cut-block, (C) interlayering of white and dark green microcline veins (K-Fsp) with charoitite (Cht) in a natural outcrop. Reactional snow-white microcline is seen between massive microcline and charoitite in figure B. A hammer with 50-cm long handle is shown in figures B and C for the scale.

3. Results

3.1. Igneous stages

3.1.1. Early intrusive stage

None of the three measured samples of the early stage intrusions yielded plateau spectrum on the argon release diagram (Fig. 5). Phlogopite from the sample Cha 1/225a shows 6 steps within their analytical errors with the weighted age value of 134.26 ± 0.32 Ma and consistent isochron age value with atmospheric argon initial ratio. Similarly, biotites from samples Cha126 and Cha 233 show sub-plateau age values of 133.14 ± 0.45 Ma and 135.17 ± 0.91 Ma, respectively. However, the amount of released ^{39}Ar is <60%, which does not allow considering the obtained age values as estimates of the true crystallization age of the intrusions.

Preprints (www.preprints.org) | NOT PEER-REVIEWED | Posted: 19 November 2018 doi:10.20944/preprints201811.0470.v1

Peer-reviewed version available at Minerals 2018, 8, 602; doi:10.3390/min8120602

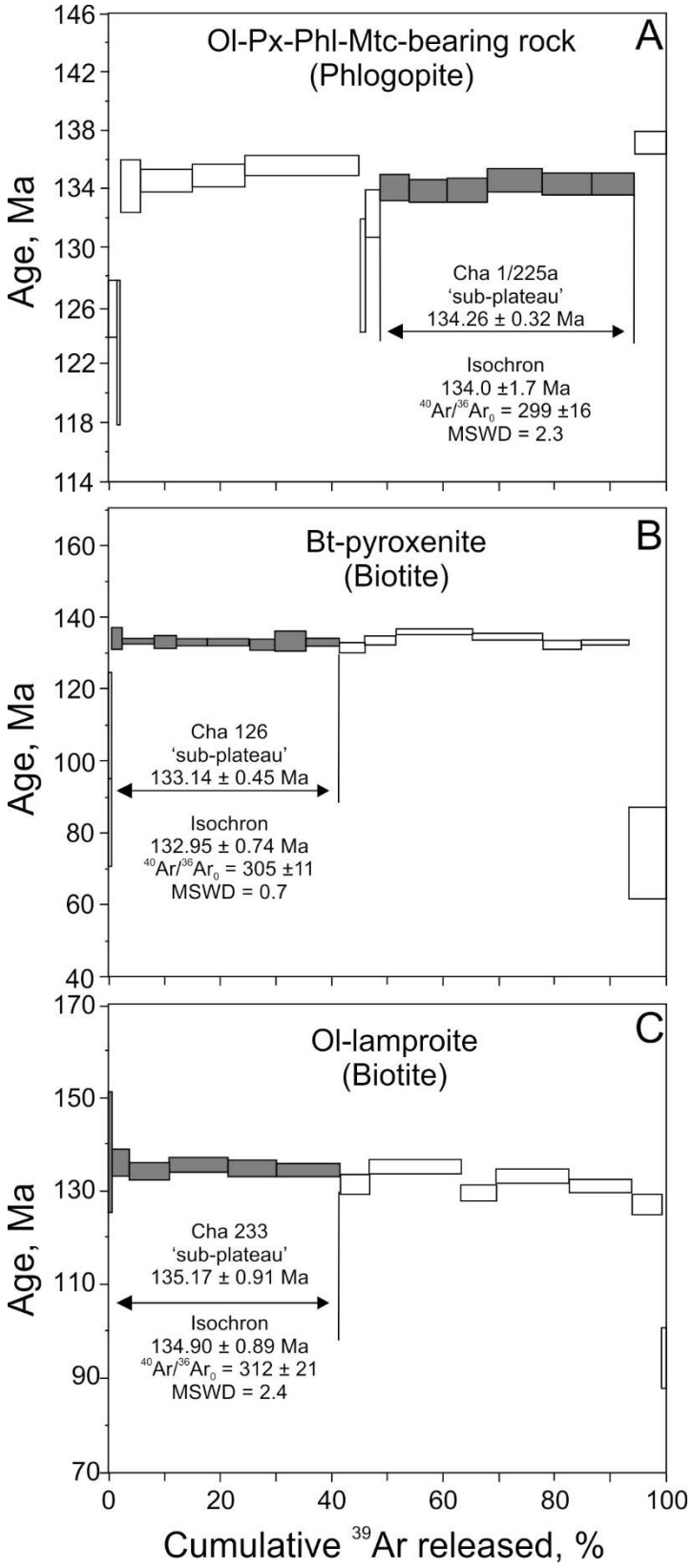

Figure 5. Argon release spectra for the early stage intrusions: (A) sample Cha1/225a – cumulative olivine-pyroxene-phlogopite-monticellite rock, (B) sample Cha126 – biotite-pyroxenite and (C) sample Cha233 – olivine lamproite. Steps used for calculation of sub-plateu and isochron age values are shadowed.

3.1.2. Main intrusive and volcanic stages

Biotite from the volumetrically predominant biotite-pyroxene syenite (alkaline syenite according to notion of Russian geologists) yielded well defined plateau with an age value of 135.76 ± 0.68 Ma and consistent isochron age value with atmospheric argon initial ratio (Fig. 6A). Biotite from leucite lamproite lava shows no plateau, but its argon release spectrum is flattened. We calculate an average of 142.66 ± 0.70 Ma for 13 steps, which is consistent with the isochron age value (Fig. 6B). Biotite from a small lujavrite intrusion yielded a plateau age value of 136.60 ± 0.88 Ma with consistent isochron age value and atmospheric isotopic composition of initially trapped argon (Fig. 6C).

3.1.3. Late intrusive stage

K-feldspar separates from benstonite and calcite carbonatites yielded plateau age values of 128.92 ± 0.80 Ma and 129.56 ± 0.76 Ma, respectively (Fig. 7A,B). These are statistically undistinguishable from each other, though calcite carbonatites cut through benstonite carbonatites (Fig. 3B). Tinaksite from another benstonite carbonatite sample yielded sub-plateau (only 3 steps) with similar, though slightly older age value of 130.93 ± 0.79 Ma (Fig. 3C).

3.2. Kedroviy stock

Strontian potassicrichrerite from a metasomatic contact of alkaline granite of the Kedroviy stock yielded a plateu with age value of 128.5 ± 1.1 Ma (Fig. 8A). In inverse isochron coordinates ($^{36}Ar/^{40}Ar$ vs $^{39}Ar/^{40}Ar$), all point plot within their errors near $^{39}Ar/^{40}Ar$ axis that does not allow to draw a linear regression throug the points. It does not affect the age calculations, but prohibits estimation of initially trapped argon isotope composition. We assign this age value to the true age of the alkaline granite intrusion.

K-feldspar from a quartz-feldspar-brookite hydrothermal vein developed in vicinity of the Kedroviy stock did not yield a plateau. All steps scatter near an average of 123.3 ± 0.3 Ma (Fig. 8B). Isochron age value is consistent with this value and show atmospheric isotopic ratio for initially trapped argon.

3.3. Charoitite complex

K-feldspar from different types of microcline monomineralic rocks yield statistically different age values. For example, granular K-feldspar from association with charoite (shown in Fig. 4A) yields a well-defined plateau age value of 126.8 ± 1.1 Ma (Fig. 9A). K-feldspar of a museum sample dated in our previous study [40] also shows well defined plateau, but with significantly different age value of 135.79 ± 0.42 Ma (Fig. 9B). This sample represents massive microclines such as shown in Fig. 4B. K-feldspar from a sample of microcline veins (such as in Fig. 4C) shows slightly disturbed age spectrum with a sub-plateau age value of 129.43 ± 0.87 Ma (Fig. 9C), which is intermediate between the age values obtained for two other samples.

Tokkoite from a museum sample of charoitite yielded a plateau age value of 135.93 ± 0.49 Ma (Fig. 10A), which is statistically indistinguishable from age value obtained for K-feldspar from massive microcline monomineralic rock (Fig. 9B). For the purpose of this study, we reirradiated tokkoite from the same museum sample. It also shows a plateau, but wit slightly younger age value of 133.9 ± 1.4 Ma (Fig. 10B). However, in inverse isochron coordinates the plateau steps show strongly non atmospheric isotopic composition of trapped argon ($^{40}Ar/^{39}Ar = 184 \pm 57$) and, thus, isochron age value became slightly older (135.9 ± 1.4 Ma) in full agreement with the age value obtained in our previous study [40].

Tinaksite from a museum sample of charoitite analysed in study [40] yielded a plateau age value of 135.86 ± 0.43 Ma (Fig. 11A) in full agreement with age values on K-feldspar from massive microcline monomineralic rock (Fig. 9B) and tokkoite (Fig. 10A,B). Large errors for isotopic composition of initially trapped argon are due to location of all points close to the x-axis ($^{39}Ar/^{40}Ar$) of the inverse isochron plot.

Preprints (www.preprints.org) | NOT PEER-REVIEWED | Posted: 19 November 2018 doi:10.20944/preprints201811.0470.v1

Peer-reviewed version available at Minerals 2018, 8, 602; doi:10.3390/min8120602

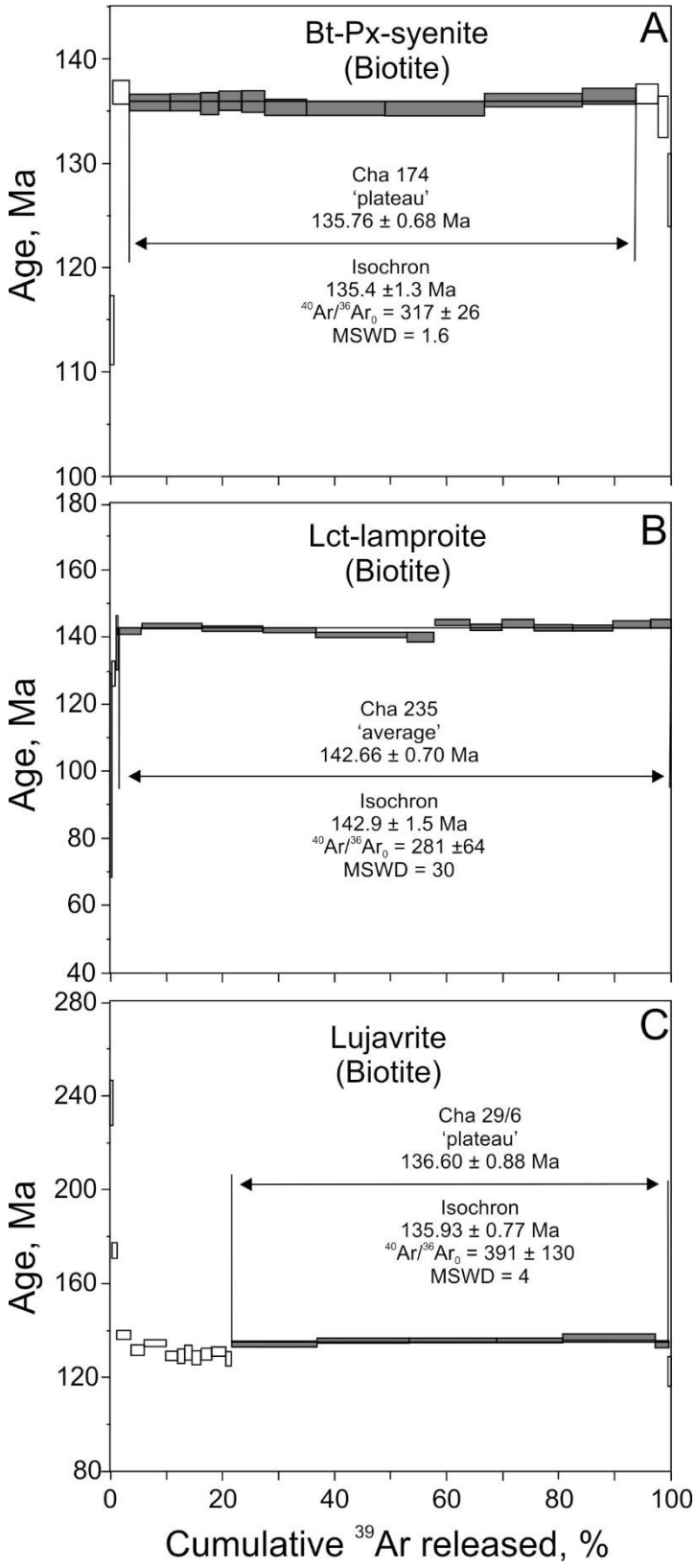

Figure 6. Argon release spectra for intrusions and lava of the main and volcanic stages: (A) sample Cha174 – biotite-pyroxene-syenite, (B) sample Cha235 – leucite lamproite and (C) sample Cha29/6 – lujavrite. Steps used for calculation of plateau, average and isochron age values are shadowed.

Preprints (www.preprints.org) | NOT PEER-REVIEWED | Posted: 19 November 2018 doi:10.20944/preprints201811.0470.v1

Peer-reviewed version available at Minerals 2018, 8, 602; doi:10.3390/min8120602

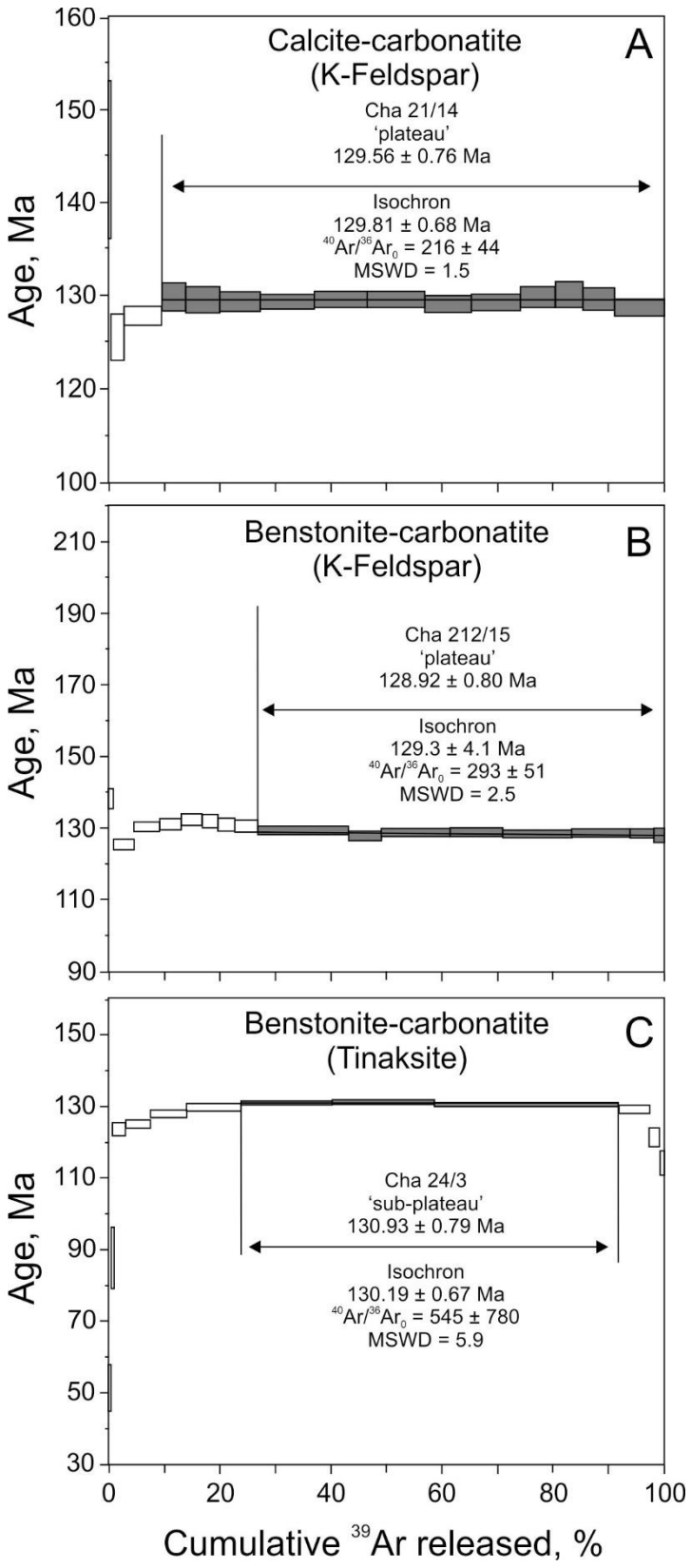

Figure 7. Argon release spectra for carbonatites of the late intrusive stage: (A) sample Cha21/14 –K-feldspar from calcite carbonatite, (B) sample Cha212/15 – K-feldspar from benstonite carbonatite and (C) sample Cha24/3 – tinaksite ($NaK_2Ca_2TiSi_7O_{19}(OH)$) from benstonite carbonatite. Steps used for calculation of plateau sub-plateu and isochron age values are shadowed.

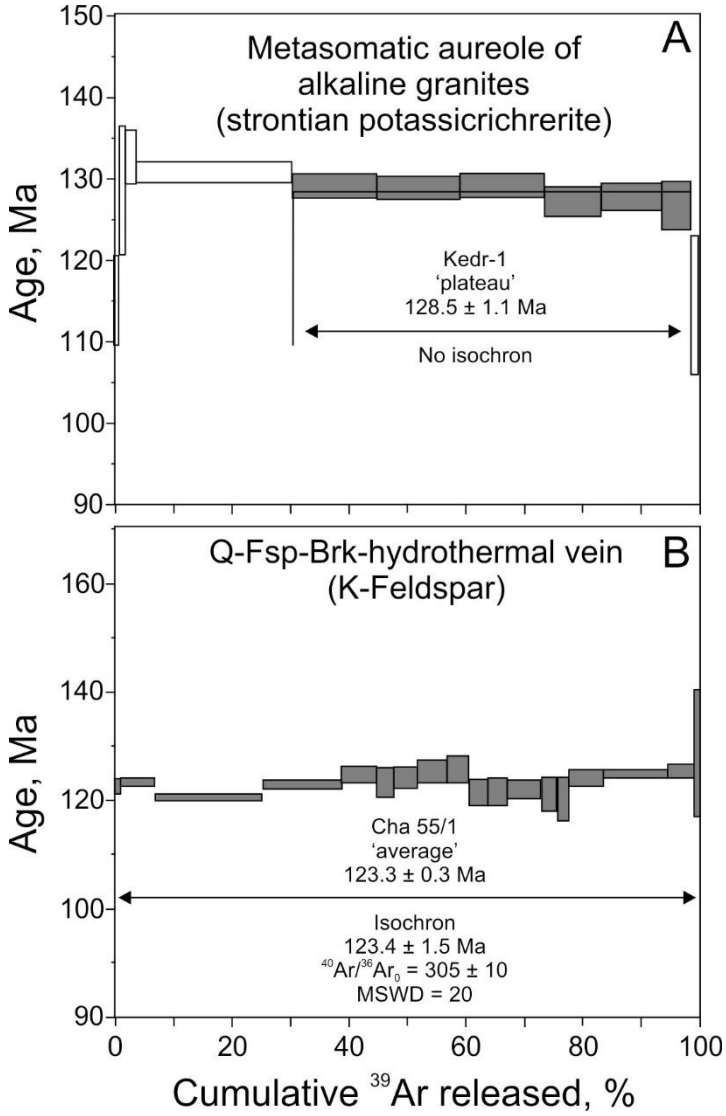

Figure 8. Argon release spectra for metasomatic and hydrothermal minerals: (A) sample Kedr-1 – strontian potassicrichrerite ($K[(Ca,Sr)Na][Mg_5]Si_8O_{22}(OH)_2$) in a contact zone of alkaline granite intrusion, (B) sample Cha55/1 – K-feldspar from quartz-feldspar-brookite hydrothermal vein. Steps used for calculation of plateau, average and isochron age values are shadowed.

K-arfvedsonite of a charoitite sample Cha117/3 yielded a well defined plateau with age value of 133.11 ± 0.34 Ma (Fig. 11B), which is intermediate between few age values at about 136 Ma for tinaksite and tokkoite and an age value of ~126 Ma obtained for granular K-feldspar in association with charoite.

Frankamenite of a museum charoitie sample analysed in [40] yielded a sub-plateau age value of 137.55 ± 0.46 Ma (Fig. 12A), which, so far, is the oldest among age values obtained for minerals of the charoitite complex. Frankamenite from the same sample reanalysed in this study show similar argon-release pattern, however, no steps can be groupped as either plateau or sub-plateau. The oldest measured age value for a single step of this sample is 133.95 ± 0.77 Ma (Fig. 12B). Frankamenite of another charoitite sample yielded a sub-plateau age value of 135.1 ± 1.7 Ma (Fig. 12C).

Preprints (www.preprints.org) | NOT PEER-REVIEWED | Posted: 19 November 2018 doi:10.20944/preprints201811.0470.v1

Peer-reviewed version available at Minerals 2018, 8, 602; doi:10.3390/min8120602

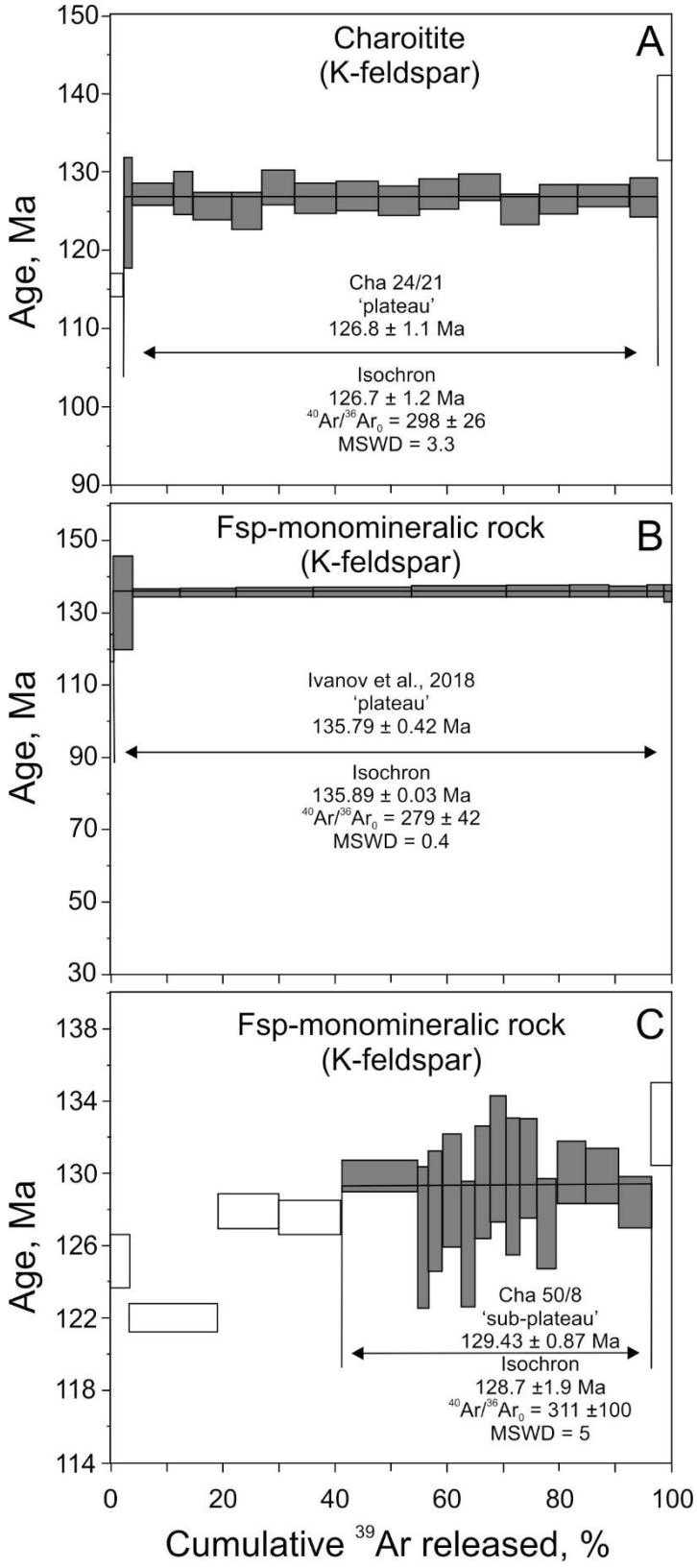

Figure 9. Argon release spectra for K-feldspar of different rocks of the charoitite complex: (A) sample Cha 24/21 – K-feldspar from charoitite, (B) museum sample of massive microclinite [40] and (C) sample Cha50/8 – K-feldspar from a microcline vein. Steps used for calculation of sub-plateau, plateau and isochron age values are shadowed.

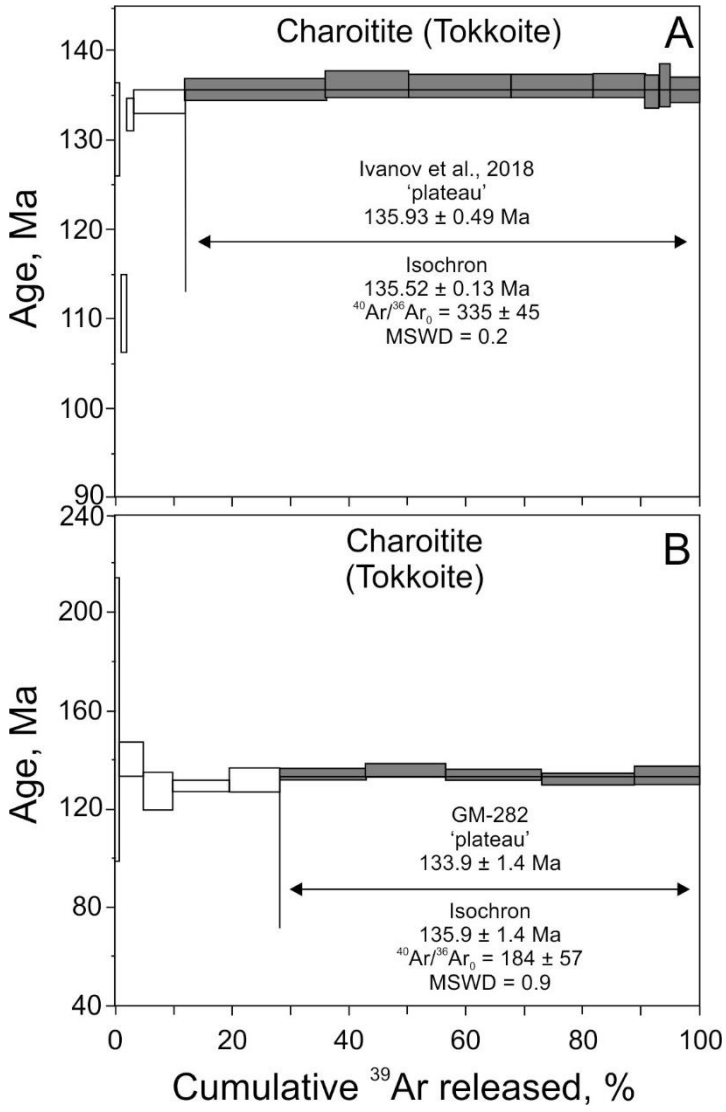

Figure 10. Argon release spectra for two different crystals of tokkoite ($K_2Ca_4Si_7O_{17}(O,OH,F)_4$) of a museum charoitite sample: (A) obtained in [40] and (B) in this study. For the sample dated in this study the isochron age is preffered due to non-atmospheric trapped argon. Steps used for calculation of plateau and isochron age values are shadowed.

4. Discussion

4.1. Timing of Cretaceause alkaline magmatism of the Aldan Shield and Transbaikalia

Age of the Malyy Murun magmatism was considered as Early Cretaceause based on K-Ar dating of biotite, K-feldspar and pyroxene separates from feldspar-calcilitic and biotite-pyroxene-K-feldspar (referred to as alkaline) syenites of the main intrusive stage [38]. Using original data from [38] and conventional ^{40}K decay constants [42], Wang et al. [39] recalculated the mean age value for syenites of the main stage as 131 ± 2.4 Ma, excluding few age values, which they considered as outliers. This mean age value is younger than the new $^{40}Ar/^{39}Ar$ age value (135.76 ± 0.68 Ma) obtained for the main stage biotite-pyroxene-K-feldspar syenite even considering the systematic difference of the order of 0.9% between ages by [39] and this study due to different ^{40}K decay constants used. We give the priority in interpretation of the geochronological data for our new $^{40}Ar/^{39}Ar$ results over refined K-Ar results of [38, 39].

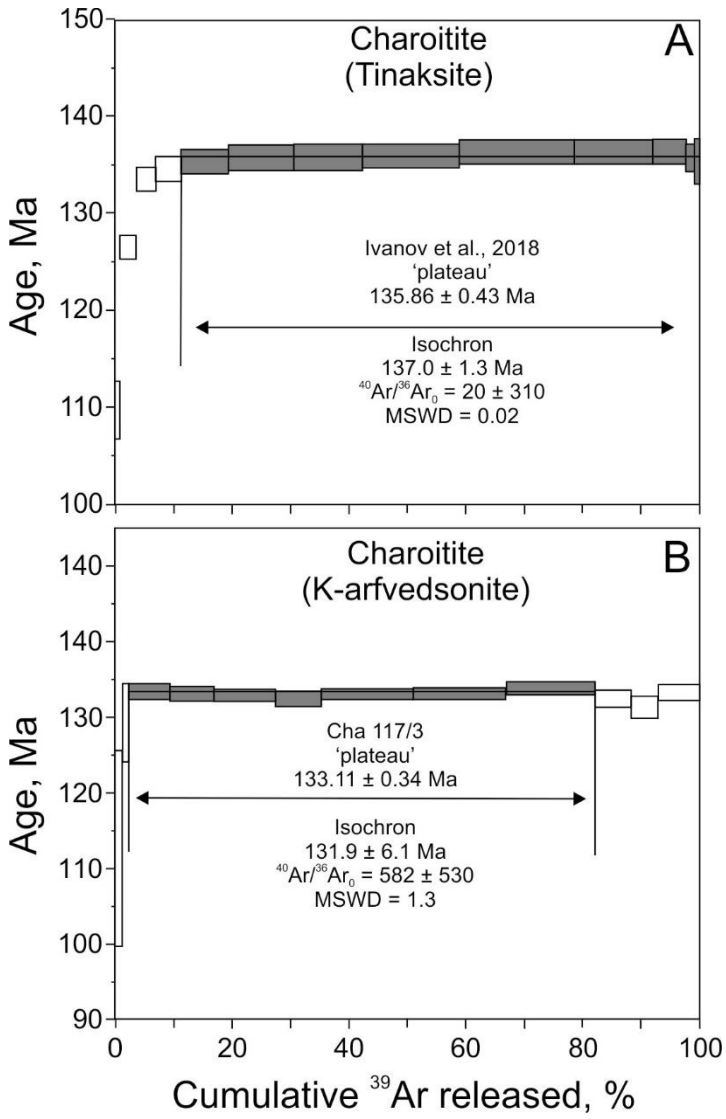

Figure 11. Argon release spectra for two different minerals of charoitites: (A) tinaksite ($NaK_2Ca_2TiSi_7O_{19}(OH)$) of a museum charoitite sample analysed in [40] and (B) K-arfvedsonite analysed in this study. Steps used for calculation of plateau and isochron age values are shadowed.

In this study, we clearly see at least two episodes of magmatism within the Malyy Murun massif defined by the plateau age values: ~135-137 Ma for the main intrusive and volcanic stages and ~128-130 Ma for the late intrusive stage (Fig. 13). The former is mainly composed by variable syenites. The latter is represented by low volume carbonatitic and alkaline granitic intrusions. With the present amount of dated samples, however, it is impossible to conclude if these were two separate episodes of magmatism, or there was continueous magmatic activity between 137 and 128 Ma. For example, the rocks of presumably early intrusive stage may indeed be younger than the main phase syenites (Fig. 13). It cannot be excluded also, that similar rocks could form during different episodes of the igneous complex development. We cannot determine either, if magmatism started at about 137 Ma or earlier, having in mind an older (~142 Ma) age value for pseudo-leucite lamproite lava (Fig. 13).

Early Cretaceous alkaline magmatism and associated ore deposits were widespread within the Aldan shield of the Siberian Craton and its surrounding along the Mongolia-Okhotsk sutute zone (Fig. 1). This magmatism and ore formation mark the post collisional extension, which occurred 40-60 million years after the supposed closure of the Mongolia-Okhotsk Ocean and peak of orogeny in Early-Middle Jurassic [e.g. 49-50]. For example, available Rb-Sr, $^{40}Ar/^{39}Ar$ and U-Pb age values for Transbaikalian volcanic rocks limit the Early Cretaceous rift-related volcanism to an interval of 133-104 Ma [51-54], whereas K-Ar age values suggest a wider age interval of 150-100 Ma [55-56]. Oshurkov massif is the best studied in Transbaikalia (Fig. 1). It contains granites, syenites, gabbro

Preprints (www.preprints.org) | NOT PEER-REVIEWED | Posted: 19 November 2018 doi:10.20944/preprints201811.0470.v1

Peer-reviewed version available at Minerals 2018, 8, 602; doi:10.3390/min8120602

and lamprohyric rocks, and carbonatites [52]. The oldest among them is leucocratic granite (132.8 ± 0.66 Ma by U-Pb SHRIMP on zircon), the youngest is granitic pegmatite (111.6 ± 1 Ma by $^{40}Ar/^{39}Ar$ on amphibole), with numerous ages obtained by Rb-Sr, $^{40}Ar/^{39}Ar$ and U-Pb methods for other rock types in between of these two [52].

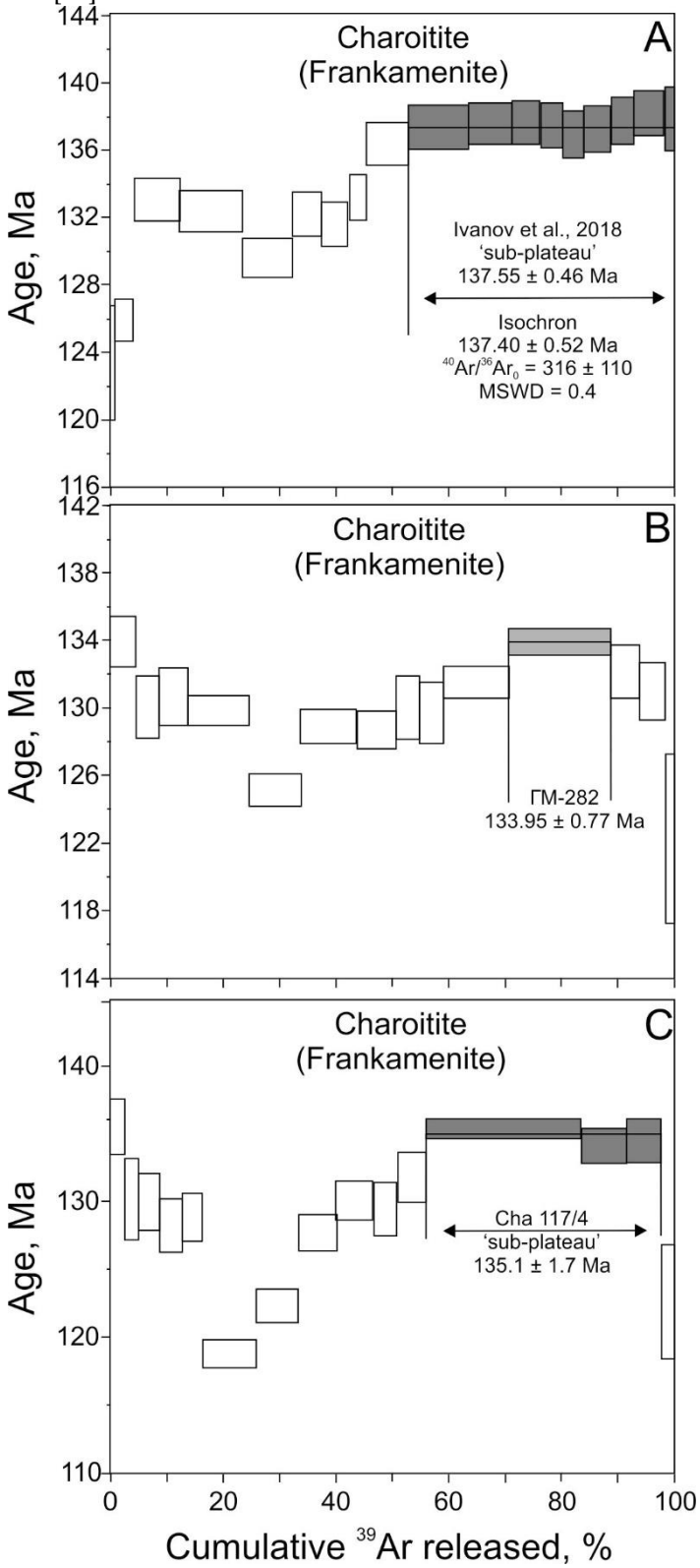

Figure 12. Argon release spectra for frankamenite ($Ca_5Na_3K_3(Si_{12}O_{30})F_3OH{\cdot}nH_2O$) crystals of two different charoitite samples: (A) obtained in [40], (B) frankamnite from the same museum sample reanalysed in this study ab (C) frankamnite from another sample Cha 117/4. Steps used for calculation of sub-plateau and single step age values are shadowed.

Preprints (www.preprints.org) | NOT PEER-REVIEWED | Posted: 19 November 2018 doi:10.20944/preprints201811.0470.v1

Peer-reviewed version available at Minerals 2018, 8, 602; doi:10.3390/min8120602

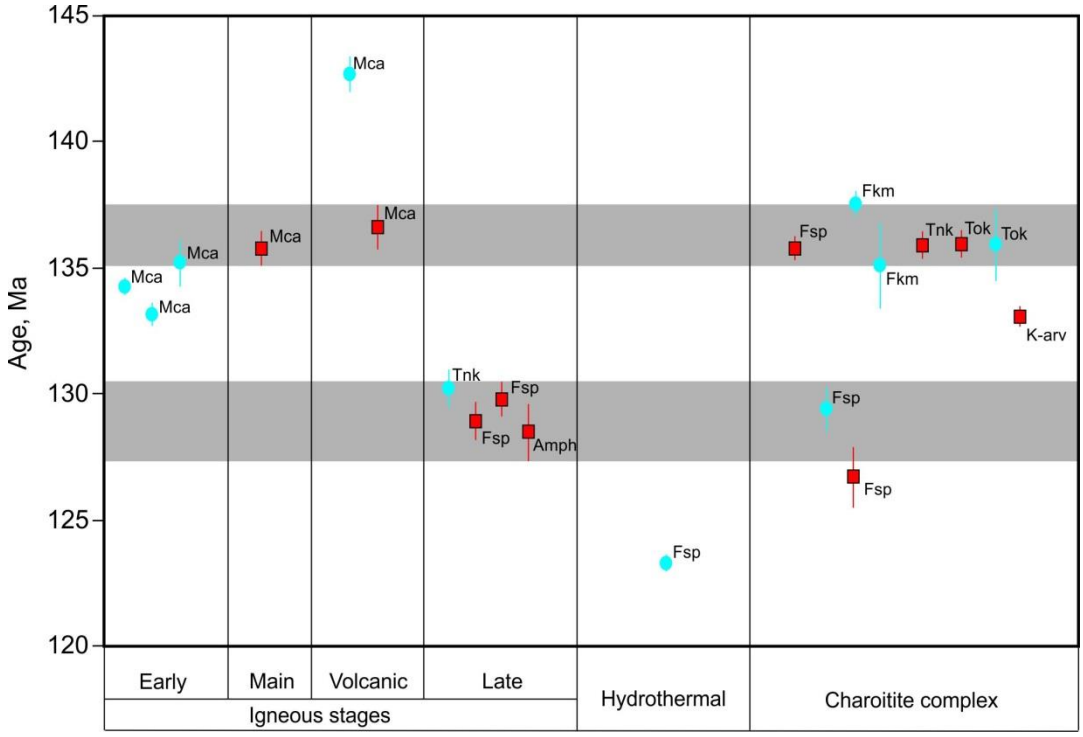

Figure 13. Summary of $^{40}Ar/^{39}Ar$ age values for the Malyy Murun massif (see Appendix A). Red squares and blue circles denote the plateau and sub-plateau/isochron age values, respectively. Horizontal grey bands show the reliably dated intervals of igneous activity within the Malyy Murun massif. Abbreviations for dated minerals: Mca – mica (biotite in most cases and phlogopite for some early stage intrusions), Fsp – K-feldspar, Amph – amphibole (strontian potassicrichrerite), Tnk – tinaksite, Tok – tokkoite, Fkm – frankamenite, K-arv – K-arvfedsonite.

Similarly, according to K-Ar dating there was an Early Cretaceous alkaline magmatism within the Aldan shield, which was also linked to rifting [38], though there were no rift basins developed. $^{40}Ar/^{39}Ar$ and U-Pb studies are rare for the Early Cretaceous alkaline intrusives of the Aldan shield, however. It seems that alkaline massifs located in the northern part of the Aldan shield are coeval; Malyy Murun – 137-128 Ma (this study); Inagly – 142-128 Ma [57]. Whereas volcanic fields and intrusions located in the southern and eastern part of the Aldan shield are generally younger and fall into an interval of 126-115 Ma [58-60]. But such geralization needs additional geochronologic studies.

4.2. The charoitite complex

The charoitite complex contains a number of unique and rare minerals, which either were not discovered anywhere else (i.e. charoite, tokkoite, frankamenite) or only were found at one or two other world localities (i.e. tinaksite and fedorite). The general opinion is that the charoitite complex is metasomatic in origin [61]. However, the alternative point of view is that charoitite is of magmatic origin and associated with evolution of lamproite and carbonatite melts [14-15].

Direct $^{40}Ar/^{39}Ar$ dating of charoite has shown that this mineral does not retain radiogenic argon due to its fibrous structure and thus its age was assessed indirectly by laser ablation $^{40}Ar/^{39}Ar$ dating on associated K-feldspar and tinaksite [39]. Individual laser ablation analyses revealed a set of age values from 134.1 ± 2.9 Ma to 113.3 ± 3.4 Ma for K-feldspar and from 133.0 ± 3.0 Ma to 115.7 ± 4.3 Ma for tinaksite [39]. The oldest and youngest ages have been interpreted as the true crystallization ages and the time for cessation of hydrothermal activity, respectively. In the present and a related study [40] we applied stepwise-heating $^{40}Ar/^{39}Ar$ dating on K-feldspar, tinaksite, tokkoite, frankamenite, fedorite and K-arvfedsonite. Fedorite have shown a staircase argon release pattern with significant radiogenic argon loss similar to charoite (and due to such effect is not discussed here). Frankamenite

have shown disturbed age spectra (Fig. 12). All other minerals have shown plateau age values (Figs. 9-11), which vary from ~136 Ma to ~127 Ma (Fig. 13). Thus, the charoitite complex was not formed at once. Its constituent minerals crystallized during the entire range of the Malyy Murun magmatism.

Geochronological data alone do not provide the final word in the discussion of metasomatic versus magmatic origin of charoitites. We wish to note, however, that the prolonged crystallization of minerals of charoitites would rather be more consistent with the interpretation of the charoitite complex as fenites originated due to interaction of alkalic magma fluid with carbonate and clastic sedimentary rocks [62].

The hydrothermal activity was dated via analyzing K-feldspar from the quartz-feldspar-brookite vein of the Kedroviy stock [19]. This K-feldspar did not yield a plateau, but its flattened argon release pattern suggests that it crystallized around 123 Ma (Fig. 8B). The hydrothermal activity could last even longer until ~113 Ma as suggested by laser ablation $^{40}Ar/^{39}Ar$ dating of K-feldspar and tinaksite for the charoitite complex [39].

5. Conclusions

The Malyy Murun massif was formed at about 137-128 Ma and it was one of many alkaline intrusive massifs and lavas emplaced in Early Cretaceous within the extensional tectonic framework of the Aldan shield and Transbaikalia.

Unique and rare minerals of the charoitite complex were not crystallized at once. Their $^{40}Ar/^{39}Ar$ age values are fully consistent with the range of age values obtained for igneous rocks of the Malyy Murun massif.

Hydrothermal activity within the Malyy Murun massif, which played an important role in remobilization of ore components, continued for several million years after the cessation of the igneous activity.

Supplementary Materials: The following are available online at www.mdpi.com/xxx/s1, Table S1: $^{40}Ar/^{39}Ar$ data.

Author Contributions: A.V.I.; methodology, investigation, data curation, funding acquisition, project administration, writing - original draft preparation. N.V.V.; resources, investigation, funding acquisition, project administration. E.I.D.; investigation, project administration, writing - original draft preparation. V.A.G.; data curation, investigation. E.Y.D.; investigation, resources.

Funding: The geochronological work was supported by a joint grant of the Russian Foundation for Basic Research and the Administration of the Irkutsk Region (no. 17-45-388067) given to A.V.I., E.I.D., V.A.G. and N.V.V. Sample collection and preparation were conducted under financial aid from grants of the Russian Foundation for Basic Research no. 17-55-45028 and no. 18-05-00073 given to N.V.V. and E.Y.D.

Acknowledgments: We thank Pavel Lomyga for providing useful geological information and Mikhail Mitichkin and Larisa Ivanova for support with museum sample collections.

Conflicts of Interest: The authors declare no conflict of interest.

Appendix A. Summary of geochronological results.

Rock name/intrusive stage, complex	Dated mineral	Preferred $^{40}Ar/^{39}Ar$ age value
Olivine-pyroxene-phlogopite-monticellite rocks/Early intrusive stage	Phlogopite	134.26 ± 0.32 Ma (sub-plateau)
Biotite-pyroxenite/Early intrusive stage	Biotite	133.14 ± 0.45 Ma (sub-plateau)
Olivine-lamproites/Early intrusive stage	Biotite	135.17 ± 0.91 Ma (sub-plateau)
Biotite-pyroxene-syenite (alkaline syenite)/Main intrusive stage	Biotite	135.76 ± 0.68 Ma (plateau)
[1]Leucite-lamproite/Volcanic stage	Biotite	142.66 ± 0.70 Ma (average)
Lujavrite/Volcanic stage	Biotite	136.60 ± 0.88 Ma (plateau)
Calcite-carbonatite/Late intrusive stage	K-feldspar	129.56 ± 0.76 Ma (plateau)
Benstonite-carbonatite/Late intrusive stage	K-feldspar	128.92 ± 0.80 Ma (plateau)
	Tinaksite	130.93 ± 0.79 Ma (sub-plateau)
Alkaline granite/Late intrusive stage	Strontian potassicrichterite	128.5 ± 1.1 Ma (plateau)
Charoitite/Charoitite complex	K-feldspar	126.8 ± 1.1 Ma (plateau)
		135.93 ± 0.49 Ma (plateau)
		135.9 ± 1.4 Ma (isochron)
	Tokkoite	135.86 ± 0.43 Ma (plateau)
	Tokkoite	133.11 ± 0.34 Ma (plateau)
	Tinaksite	137.55 ± 0.46 Ma (sub-plateau)
	K-arfvedsonite	135.1 ± 1. 7 Ma (sub-plateau)
	Frankamenite	133.95 ± 0.77 Ma (oldest step)
	Frankamenite	135.79 ± 0.42 Ma (plateau)
	Frankamenite	129.43 ± 0.87 Ma (sub-plateau)
Microcline monomineralic rock/Charoitite complex	K-feldspar	123.3 ± 0.3 (average)
	K-feldspar	
Quartz-feldspar-brookite-vein	K-feldspar	

[1] Leucite in all rocks is recrystallized and identified by its crystal morphology.

References

1. Vladykin, N.V. 1ST occurrence of lamproites in the USSR. *Doklady Akademii Nauk SSSR* **1985**, 280, 718-722.
2. Prokofev, V.Y.; Vorobiov, E.I. P-T conditions of formation of the Sr-Ba carbonatites, chariots, and torgolites of Murunsky alkaline massif (Eastern Siberia). *Geochimiya* **1991**, 10, 1444-1452.

3. Mitchell, R.H.; Smith, C.B.; Vladykin, N.V. Isotopic composition of strontium and neodymium in potassic rocks of the Little Murun complex, Aldan Shield, Siberia. *Lithos* **1994**, 32, 243-248, DOI 10.1016/0024-4937(94)90042-6.
4. Panina, L.I. Low-titanium Aldan lamproites (Siberia): Melt inclusions in minerals. *Geoloiya i Geofizika* **1997**, 38, 112-122.
5. Konev, A.A.; Feoktistov, G.D. Genesis of ultrasilicic alkaline granitoids. *Petrology* **1998**, 6, 62-69.
6. Panina, L.I.; Usol'tseva, L.M. The role of liquid immiscibility of calcitic carbonatites from the Malyi Murun Massif (Aldan). *Geoloiya i Geofizika* **2000**, 41, 655-670.
7. Vladykin, N.V. The Malyi Murun volcano-plutonic complex: An example of differentiated mantle magmas of lamproitic type. *Geochemistry International* **2000**, 38, S73-S83.
8. Sokolov, S.V.; Sidorenko, G.A.; Chukanov, N.V.; Chistyakova, N.I. On benstonite and benstonite carbonatites. *Geochemistry International* **2001**, 39, 1218-1229.
9. Davies, G.R.; Stolz, A.J.; Mahotkin, I.L.; Nowell, G.M.; Pearson, D.G. Trace element and Sr-Pb-Nd-Hf isotope evidence for ancient, fluid-dominated enrichment of the source of Aldan shield lamproites. *Journal of Petrology* **2006**, 47, 1119-1146, DOI 10.1093/petrology/egl005.
10. Markl, G.; Marks, M.A.W.; Frost, B.R. On the controls of oxygen fugacity in the generation and crystallization of peralkaline melts. *Journal of Petrology* **2010**, 51, 1831-1847, DOI 10.1093/petrology/egq040.
11. Reguir, E.P.; Chakhmouradian, A.R.; Pisiak, L.; Halden, N.M.; Yang, P.; Xu, C.; Kynicky, J.; Coueslan, C.G. Trace-element composition and zoning in clinopyroxene- and amphibole-group minerals: Implications for element partitioning and evolution of carbonatites. *Lithos* **2012**, 128, 27-45, DOI 10.1016/j.lithos.2011.10.003.
12. Vorob'ev, E.I. Strontium-barium carbonatites of the Murun massif (Eastern Siberia, Russia). *Geology of Ore Deposits* **2001**, 43, 468-480.
13. Vladykin, N.V.; Tsaruk, I.I.. Geology, chemistry, and genesis of Ba-Sr-bearing ("benstonite") carbonatites of the Murun Massif. *Geoloiya i Geofizika* **2003**, 44, 325-339.
14. Vladykin, N.V.; Viladkar, S.G.; Miyazaki, T.; Mohar, V.R. Geochemistry of benstonite and associated carbonatites of Sevathur, Jogipatti and Samalpatti, Tamil Nadu, South India and Murun Massif, Siberia. *Journal of the Geological Society of India* **2008**, 72, 312-324.
15. Vladykin, N.V. Potassium alkaline lamproite-carbonatite complexes: petrology, genesis, and ore reserves. *Russian Geology and Geophysics* **2009**, 50, 1119-1128, DOI: 10.1016/j.rggg.2009.11.010.
16. Vladykin, N.V. Genesis and crystallization of ultramafic alkaline carbonatite magmas of Siberia: ore potential, mantle sources, and relationship with plume activity. *Russian Geology and Geophysics* **2016**, 57, 698-712, DOI 10.1016/j.rgg.2015.09.014.
17. Borisenko, A.S.; Borovikov, A.A.; Vasyukova, E.A.; Pavlova, G.G.; Ragozin, A.L.; Prokop'ev, I.R.; Vladykin, N.V. Oxidized magmatogene fluids: metal-bearing capacity and role of ore formation. *Russian Geology and Geophysics* **2011**, 52, 144-164, DOI 10.1016/j.rgg.2010.12.011.
18. Makar'ev, L.B.; Mironov, Yu.B.; Kukharenko, E.A.; Sharpenok L.N. Breccias formation in Mesozoic ultrapotassic alkaline rocks of the Murunsky magmatic cluster (Northern Transbaikal). *Regional Geology and Metallogeny* **2016**, 66, 45-52.
19. Borovikov, A.A.; Vladykin, N.V.; Tretiakova, I.G., Dokuchits, E.Y. Physicochemical conditions of formation of hydrothermal mineralization on the Murunskiy alkaline massif, western Aldan (Russia). *Ore Geology Reviews* **2018**, 95, 1066-1075, DOI 10.1016/j.oregeorev.2017.11.007.
20. Rogova, V.P.; Rogov, Y.G.; Drits, V.A.; Kuznetsova, N.I.; Charoite – a new mineral and new jewelry-stone. *Zapiski Vsesoyuznogo Mineralogicheskogo Obshchestva* **1978**, 1, 94–100.
21. Konev, A.A.; Vorobyev, E.I.; Lazebnik, K.A., 1996, *Mineralogy of the Murun alkaline massif*; NITS OIGGIM: Novosibirsk, Russia, 1996, pp. 1-221, ISBN 5-7692-0006-5.
22. Vorobyev, E.I. *Charoite*; Academic Publisher "GEO": Novosibirsk, Russia, 2008, pp. 1-140, ISBN 978-5-9747-0116-0.
23. Shevelev, A.S., editor. *Charoite. Violet marvel of Siberia*, 2nd ed.; Petrographica: Irkutsk, Russia, 2013, pp. 1-191, ISBN 978-5-4337-0013-0.
24. Shevelev, A.S. *Baikalian gemstones. An illustrated science-popular publication*; Petrographica: Irkutsk, Russia, 2017, pp. 1-176, ISBN 978-5-9908900-6-0.
25. Rozhdestvenskaya, I.; Mugnaioli, E.; Czank, M.; Depmeier, W.; Kolb, U.; Reinholdt, A.; Weirich, T.; The structure of charoite, $(K,Sr,Ba,Mn)_{15-16}(Ca,Na)_{32}[(Si_70(O,OH)_{180})](OH,F)_{4.0}{}^*nH_2O$, solved by conventional and automated electron diffraction. *Mineralogical Magazine* **2010**, 74, 159–177, DOI 10.1180/minmag.2010.074.1.159.

26. Rogov, Yu.G.; Rogova, V.P.; Voronkov, A.A.; Moleva, V.A. Tinaksite $NaK_2Ca_2TiSi_7O_{19}(OH)$ – a new mineral. *Doklady Akademii Nauk SSSR* **1965**, 162, 658-661.
27. Lacalamita, M.; Mesto, E..; Kaneva, E.; Scordari, F.; Pedrazzi, G.; Vladykin, N.; Schingaro, E. Structure refinement and crystal chemistry of tokkoite and tinaksite from the Murun massif (Russia). *Mineralogical Magazine* **2017**, 81, 251-272, DOI 10.1180/minmag.2016.080.094.
28. Lazebnik, K.A.; Nikishova, L.V.; Lazebnik, Y.D. Tokkoite a new mineral of charoitites. *Mineralogicheskii Zhurnal* **1986**, 8, 85-89.
29. Nikishova, L.V.; Lazebnik, K.A.; Rozhdestvenskaya, I.V.; Emel'yanova, N.N.; Lazebnik, Yu.D. Frankamenite K2Na3Ca5(Si12O30)F3(OH)H2O – a new mineral, triclinic variety of canasite from charoitites. *Zapiski Vsesoyuznogo Mineralogicheskogo Obschestva* **1996**, CXXV, 106-108.
30. Rozhdestvenskaya, I.V.; Nikishova, L.V.; Lazebnik, K.A. The crystal structure of frankamenite. *Mineralogical Magazine* **1996**, 60, 897-905, DOI 10.1180/minmag.1996.060.403.05.
31. Konev, A.A.; Paradina, L.F.; Vorob'ev, E.I.; Malyshonok, Yu.V.; Lapides, I.L.; Uschapovskaya, Z.F. Magnesiumstrontian poassicricterite - a new variety of amphiboles. *Mineralogicheskii Zhurnal* **1988**, 10, 76-82.
32. Sokolova, E.V.; Kabalov, Y.K.; McCammon, C.; Schneider, J. Konev, A.A. Cation partitioning in an unusual strontian potassicrichterite from Siberia: Rietveld structure refinement and Mossbauer spectroscopy. *Mineralogical Magazine* **2000**, 64, 19-23, DOI 10.1180/002646100549094.
33. Afonina, G.G.; Sapozhnikov, A.N.; Vorobiev, E.I.; Konev, A.A.; Maishonok, I.V. The x-ray characteristics of tausonite, a new mineral of perovskite group. *Acta Cristallographica, Section A* **1984**, 40, C249-C249, DOI 10.1107/S0108767384092540.
34. Mitchell, R.H.; Vladykin, N.V. Rare-earth element-bearing tausonite and potassium barium titanites from the Little Murun potassic alkaline complex, Yakutia, Russia. *Mineralogical Magazine* **1993**, 57, 651-664, DOI 10.1180/minmag.1993.057.389.09.
35. Dobrovol'skaya, M.G.; Tsepin A.I.; Evstigneeva, T.L. Murunskite $K_2Cu_3FeS_4$ – a new sulfide of potassium, cuprum and iron. *Zapiski Vsesoyuznogo Mineralogicheskogo Obschestva* **1981**, 4, 468-473.
36. Pekov, I.V.; Zubkova, N.V.; Lisitsyn, D.V.; Pushcharovsky, D.Yu. Crystal chemistry of murunskite. *Doklady Earth Sciences* **2009**, 424, 139-141, DOI 10.1134/S1028334X09010292.
37. Chakhmouradian, A.R.; Cooper, M.A.; Ball, N.; Reguir, E.P.; Medici, L.; Abdu, Y.A.; Antonov, A.A. Valdykinite, Na3Sr4(Fe2+Fe3+)Si8O24: a new complex sheet silicate from peralkaline rocks of the Murun complex, eastern Siberia, Russia. *American Mineralogist* **2014**, 99, 235-241, DOI 10.2138/am.2014.4528.
38. Kostyuk, V.P.; Panina, L.I.; Zhidkov, A.Y.; Orlova, M.P.; Bazarova, T.Y. *Potassic alkaline magmatism of the Baikal-Stanovoy rifting system*; Nauka: Novosibirsk, 1990, pp. 1-238, ISBN 5-02-028819-5.
39. Wang, Y.; He, H.-Y.; Ivanov, A.V.; Zhu, R.-X.; Lo, C.-H. Age and origin of charoitite, Malyy Murun massif, Siberia, Russia. *International Geology Review* **2014**, 56, 1007-1019, DOI 10.1080/00206814.2014.914860.
40. Ivanov, A.V.; Gorovoy, V.A.; Gladkochub, D.P.; Shevelev, A.S.; Vladykin, N.V. The first precise data on the age of charoite mineralization (Eastern Siberia, Russia). *Doklady Earth Sciences* **2018**, 478, 179-182, DOI 10.1134/S1028334X18020241.
41. Kiselev, A.I.; Yarmolyuk, V.V.; Ivanov, A.V.; Egorov, K.N. Middle Paleozoic basaltic and kimberlitic magmatism in the northwestern shoulder of the Vilyui Rift, Siberia: relations in space and time. *Russian Geology and Geophysics* **2014**, 55, 144-152, DOI 10.1016/j.rgg.2014.01.003.
42. Steiger, R.H.; Jager, E. Subcommission on geochronology – convention on use of decay constants in geochronology and cosmochronology. *Earth and Planetary Science Letters* **1977**, 36, 359-362, DOI 10.1016/0012-821X(77)90060-7.
43. Lee, J.-Y.; Marti, K.; Severinghaus, J.P.; Kawamura, K.; Yoo, H.-S.; Lee, J.B.; Kim, J.S.; A redetermination of the isotopic abundances of atmospheric Ar. *Geochimica et Cosmochimica Acta* **2006**, 70, 4507–4512, DOI 10.1016/j.gca.2006.06.1563.
44. Min, K.W.; Mundil, R.; Renne, P.R.; Ludwig, K.R. A test for systematic errors in $^{40}Ar/^{39}Ar$ geochronology through comparison with U/Pb analysis of a 1.1 Ga rhyoline. *Geochimica et Cosmochimica Acta* **2000**, 64, 73-98, DOI 10.1016/Soo16-7037(99)00204-5.
45. Ivanov, A.V. Systematic differences between U-Pb and $^{40}Ar/^{39}Ar$ dates: Reasons and evaluation techniques. *Geochemistry International* **2006**, 44, 1041-1047, DOI 10.1134/S0016702906100090.
46. Renne, P.R.; Mundil, R.; Balco, G.; Min, K.; Ludwig, K.R.; Joint determination of ^{40}K decay constants and $^{40}Ar^*/^{40}K$ for the Fish Canyon sanidine standard, and improved accuracy for $^{40}Ar/^{39}Ar$ geochronology. *Geochimica et Cosmochimica Acta* **2010**, 74, 5349–5367, DOI 10.1016/j.gca.2010.06.017.

47. Ivanov, A.V.; Demonterova, E.I.; Savatenkov, V.M.; Perepelov, A.B.; Ryabov, V.V.; Shevko, A.Y. Late Triassic (Carnian) lamproites from Noril'sk, polar Siberia: Evidence for melting of the recycled Archean crust and the question of lamproite source for some placer diamond deposits of the Siberian Craton. *Lithos* **2018**, 296, 67-78, DOI 10.1016/j.lithos.2017.10.021.
48. Ludwig, K.R. Isoplot 3.75. A geochronological toolkit for Microsoft Excel. *Berkeley Geochronology Center Special Publication* **2012**, 5, 1-75.
49. Donskaya, T.V.; Gladkochub, D.P.; Mazukabzov, A.M.; Ivanov, A.V. Late Paleozoic-Mesozoic subduction-related magmatism at the southern margin of the Siberian continent and the 150 million-year history of the Mongol-Okhotsk Ocean. *Journal of Asian Earth Sciences* **2013**, 62, 79-97, DOI 10.1016/j.jseaes.2012.07.023.
50. Demonterova, E.I.; Ivanov, A.V.; Mikheeva, E.M.; Arzhannikova, A.V.; Frolov, A.O.; Arzhannikov, S.G.; Bryanskiy, N.V.; Pavlova, L.A. Early to Middle Jurassic history of the southern Siberian continent (Transbaikalia) recorded in sediments of the Siberian Craton: Sm-Nd and U-Pb provenance study. *Bulletin de la Societe Geologique de France* **2017**, 188, UNSP 8, DOI 10.1051/bsgf/2017009.
51. Stupak, F.M.; Travin, A.V. The age of Late Mesozoic volcanogenic rocks of northern Transbaikalia ($^{40}Ar/^{39}Ar$ data). *Geologiya i Geofizika* **2004**, 45, 280-284.
52. Ripp, G.S.; Izbrodin, I.A.; Doroshkevich, A.G.; Lastochkin, E.I.; Rampilov, M.O.; Sergeev, S.A.; Travin, A.V.; Posokhov, V.F. Chronology of the formation of the gabbro-syenite-granite series of the Oshurkovo pluton, western Transbaikalia. *Petrology* **2013**, 21, 375-392, DOI 10.1134/S0869591113030053.
53. Ivanov, A.V.; Demonterova, E.I.; He, H.-Y.; Perepelov, A.V.; Travin, A.V.; Lebedev, V.A. Volcanism in the Baikal rift: 40 years of active-versus-passive model discussion. *Earth-Science Reviews* **2015**, 148, 18-43, DOI 10.1016/j.earscirev.2015.05.011.
54. Dash, B.; Yin, A.; Jiang, N.; Tseveendorj, B.; Han, B. Petrology, structural setting, timing, and geochemistry of Cretaceaous volcanic rocks in eastern Mongolia: Constraints on their tectonic origin. *Gondwana Research* **2015**, 27, 281-299, DOI 10.1016/j.gr.2013.10.001.
55. Ivanov, V.G.; Yarmolyuk, V.V.; Smirnov, V.N. New data on the age of volcanism evidence in the West-Zabaikalian Late Mesozoic-Cenozoic volcanic domain. *Doklady Akademii Nauk* **1995**, 345, 648-652.
56. Stupak, F.M.; Kudryashova, E.A.; Lebedev, V.A.; Gol'tsman, Y.V. The structure, composition, and conditions of generation for the Early Cretaceous Mongolia-East-Transbaikalia volcanic belt: The Durulgui-Torei area (southern Transbaikalia, Russia). *Journal of Volcanology and Seismology* **2018**, 12, 34-46, DOI: 10.1134/S0742046318010074.
57. Ponomarchuk, A.V.; Prokopyev, I.R.; Svetlitskaya, T.V.; Doroshkevich, A.G. $^{40}Ar/^{39}Ar$ geochronology of Inagly alkaline rocks (Aldan shield, south Yakutia). *Russian Geology and Geophysics* **2019**, in press.
58. Polin, V.F.; Glebovitskii, V.A.; Mitsuk, V.V.; Kiselev, V.I.; Budnitskiy, S.Y.; Travin, A.V.; Rizvanov, N.G.; Barinov, N.N.; Ekimova, N.I.; Ponomarchuk, A.V. Two-stage formation of the Alkaline volcano-plutonic complexes in the Ketkap-Yuna igneous province of the Aldan Shield: New isotopic data. *Doklady Earth Sciences* **2014**, 459, 1322-1327, DOI 10.1134/S1028334X14110051.
59. Prokoyev, I.R.; Kravchenko, A.A.; Ivanov, A.I.; Borisenko, A.S.; Ponomarchuk, A.V.; Zaitsev, A.I.; Kardash E.A.; Rozhkov, A.A. Geochronology and ore mineralization of the Dzheltula alkaline massif (Aldan Shield, South Yakutia). *Russian Journal of Pacific Geology* **2018**, 12, 34-45, DOI 10.1134/S1819714018010062.
60. Buchko, I.V.; Sorokin, A.A.; Ponomarchuk, V.A.; Kotov, A.B.; Travin, A.V.; Kovach, V.P. Trachyandesites of the Mogot volcanic field (Stanovoi volcanoplutonic belt, East Siberia): age, geochemical features, and sources. *Russian Geology and Geophysics* **2016**, 57, 1389-1397, DOI 10.1016/j.rgg.2016.01.017.
61. Charoite. Available online: https://www.mindat.org/min-972.html (accessed on 14.11.2018).
62. Lentz, D.R. Carbonaite genesis: A reexamination of the role of intrusion-related pneumatolytic skarn processes in limestone melting. *Geology* **1999**, 27, 335-338, DOI 10.1130/0091-7613(1999)027<0335:CGAROT>2.3.CO;2.